学位論文

「Papillary thyroid carcinoma with heterotopic ossification is a special subtype with extensive progression 」

（異所性骨化を伴う甲状腺乳頭癌は広範な進行を呈する特殊な亜型である）

指導教授名　岡本　牧人

申請者氏名　竹田　昌彦

著者の宣言

本学位論文は、著者の責任において実験を遂行し、得られた真実の結果に基づいて正確に作成したものに相違ないことをここに宣言する。

要旨

目的

甲状腺乳頭癌の摘出検体において、癌組織中に骨化とその近傍の結節状の線維化を認めることがしばしばあるが、その臨床病理学的意義はこれまで検討されていない。本研究のは、甲状腺乳頭癌における骨化、線維化の臨床病理学的意義と骨化症例における癌浸潤・転移メカニズムを解明するために行った。

方法

2000～2007年に北里大学病院にて切除された甲状腺乳頭癌は207例であった。そのうち病変内に骨化がみられた症例は48例、骨化はないものの結節状線維化が認められたのは26例であった。骨化も結節状線維化も認めない他の症例から34例をランダムに抽出し、これら3群の計108例と、対照として同期間に切除された33例の甲状腺濾胞癌 について臨床病理学的検討を行った。

結果

骨化あり群では全ての症例で結節状の線維化を有していた。腫瘍径は甲状腺乳頭癌の3群間で有意差を認めなかった。リンパ節転移、腺内転移、脈管浸潤、腺外浸潤は、いずれも骨化あり群において骨化・線維化なし群に比し、有意に高い頻度で認められた。背景の甲状腺組織へのリンパ球浸潤の検討では、3群間に有意差

は見られなかった。免疫染色での検討では腫瘍間質における筋線維芽細胞が骨化あり群と結節状線維化あり群において、骨化・線維化なし群に比べ有意に高密度であった。異所性骨化に関連する bFGF, BMP-2 の発現は 3 群間に有意差を認め、骨化あり群でこれらの因子を最も強く発現していた。微小血管密度は 3 群間に有意差を認めないが、nestin で検討した新生血管の密度は骨化あり群で最も高く、また腫瘍細胞での VEGF 発現も同様に骨化あり群で結果で最も強かった。

考察

甲状腺乳頭癌は甲状腺悪性腫瘍の中で最の 70%以上を占めている。近年、甲状腺乳頭癌の手術例は増加しているが、これは超音波検査や穿刺吸引細胞診などの術前診断が正確に行われるようになったことに起因している。甲状腺腫瘍の画像診断において、癌を疑う所見の 1 つとして腫瘍組織内の石灰化が知られており、その画像診断上の有用性が確立されている。実際に摘出検体において、乳頭癌組織中に骨化を認めることがあり、その近傍には結節状の線維化が存在する。しかし、その臨床病理学的意義はいままで検討されていなかった。

今回、甲状腺乳頭癌を腫瘍組織内に出現する異所骨化と線維化の有無により 3 つ型に分類し検討した。骨化あり群はリンパ節転移、脈管侵襲と腺外浸潤が高い発生率を示しており、さらに骨化あり群は結節状の線維化を前例伴っていた。そこで、

腫瘍間質に出現する筋線維芽細胞数について検討したところ、骨化あり群症例と結節状線維化あり群は結節状線維化なし群に比べて優位に多く間質中に筋線維芽細胞の出現を認め、さらに、結節状の線維化部分のみを比較したところ、結節状線維化あり群は、骨化あり群より線維化部分に筋線維芽細胞が多く見られた。これらの所見から結節状の線維化部分は時間の経過とともに硝子化し、異所性の骨化がその硝子化した古い線維性の領域に生ずるものではないかと考えられた。

腫瘍間質の線維化や異所性骨化に関連する蛋白である bFGF, BMP-2 の発現は 3 群間に有意差を認め、骨化あり群がこれらの因子を最も強く発現していたことから、腫瘍細胞がこれらの因子を発現し続けることにより、筋線維芽細胞を分化させ、間質中の線維化、骨化を促すという機構があることが示唆された。

リンパ節転移の機構について、CD34、nestin の染色によりに微小血管密度と VEGF の腫瘍細胞での発現を検討した。CD34 陽性の血管数は 3 群間に差がないにも関わらず、nestin 陽性血管数は骨化あり群で最も多いこと、同様に VEGF も骨化あり群でもっとも強く発現していることから、VEGF 産生による血管新生が骨化あり症例におけるリンパ管浸潤と関連があると考えられた。

結語

骨化あり症例は、高頻度にリンパ節転移、腺内多発と腺外浸潤を示した。

癌細胞が発現するbFGFは、筋線維芽細胞を刺激し増殖させることにより、結節状の線維化を形成させる。そして、癌細胞から分泌されるBMP-2によって、硝子化して古くなった結節状の線維化は骨化してくるものと考えられる。このような癌細胞はVEGFを産生し、血管新生とリンパ管浸潤を来たしやすい。

以上の結果より、異所性骨化を伴った甲状腺乳頭癌は、広範な進行を呈する特殊な亜型であると考える。

目次

Introduction

The presence of calcification is one of the most significant findings in ultrasonography or CT scan in evaluating thyroid nodules. Calcification is more frequently detected in papillary thyroid carcinoma than in other thyroid lesions (1). Papillary carcinoma represents the largest proportion of thyroid malignancies.

The stroma of papillary carcinoma consists of fibrous extracellular matrix and a community of stromal cells including fibroblasts, endothelium, inflammatory cells, and calcification and intratumoral heterotopic ossification (IHO). IHO is an occasional histological characteristic of papillary carcinoma. Bai et al. reported that stromal calcification was associated with pT classification and lymph node metastasis (2). However, they failed to show the clinicopathological significance of IHO in papillary carcinoma.

Tumor-stroma interaction plays an important role in tumor invasion and metastasis of digestive organ cancers (3). Papillary carcinoma frequently contains nodular fibrosis (NF). This fibrosis is composed of a mixture of fibroblasts and various amounts of collagen fiber. □□Smooth muscle actin

(□SMA) - positive fibroblasts (myofibroblasts), previously termed activated fibroblasts, are also present in areas of wound healing and chronic inflammation, and promote angiogenesis, stimulate proliferation of epithelial cells, and produce extracellular matrix, growth factors, and cytokines (4).

Basic fibroblast growth factor (bFGF) is a potent chemotactic and mitogenetic factor for smooth muscle cells and myofibroblasts (5). bFGF makes up a complex family of signaling molecules involved in several physiologic processes, and has diverse biological functions, including involvement in cellular growth, differentiation, tumor invasion, and angiogenesis (6,7).

Bone morphogenetic proteins (BMPs) are members of the transforming growth factor-□ (TGF-□) superfamily, originally described as proteins that can induce ectopic bone formation when implanted into muscle tissue *in vivo* (8). Current evidence suggests that they also participate in various biological processes of cells, such as proliferation, differentiation, and apoptosis (9). BMP-2, which is a subtype of the BMP family, has been shown to play a crucial role in the occurrence and development of breast cancer, lung cancer,

and colon cancer (10-12). However, the relationship between BMP-2 and thyroid carcinoma has not been characterized.

In the present study, we histologically classified the intratumoral fibrosis and ossification status into 3 types: papillary carcinoma (PAP) with IHO, PAP with NF, and PAP without NF. For comparison with papillary carcinomas, cases of follicular carcinoma were also examined. After the classification, clinicopathological findings were examined, and the expressions of □SMA, bFGF, and BMP-2, as well as the state of vascular proliferation were immunohistochemically analyzed, and roles of each protein in the formation of NF and IHO in thyroid papillary carcinoma were discussed.

Materials and methods

Patients and Tumor Samples

In a pathology file of Kitasato University Hospital between 2000 and 2007, 207 surgically treated cases of papillary carcinoma were included. From the 207 papillary carcinoma cases, after reviewing the histological slides, 48 cases with IHO and 26 cases with NF were totally collected. For

comparison, 34 cases without NF were selected at random. For further comparison , 33 cases of follicular carcinoma were totally collected from the file of the same period. Clinical information was obtained from the patients' medical records. All of the patients were Japanese, ranging in age from 19 to 84 years old (average, 53.6 years).

For pathological examination, the surgically resected specimens were routinely fixed in 10% buffered formalin, and the entire tumor and non-tumorous thyroid tissue were cut into slices at thicknesses of 0.3 to 0.5cm. The size and gross appearance of the tumors were recorded, and the former was validated by comparison with tumor size on histological slides. The sections were processed routinely and embedded in paraffin. One section from each of the removed lymph nodes was also processed routinely in the same way as for the thyroids.

Histological Examination

All sections were stained with hematoxylin and eosin as well as elastica van Gieson, and histopathologically examined. Histological types of thyroid carcinomas were determined according to the WHO classification (Table 2A

and 2B). IHO in papillary thyroid carcinoma was defined as lamellar bone formation in the interstitial spaces. Concerning stromal calcification, band-like calcification was recorded for a size of 1 mm or more. It was clearly differentiated from psammoma body.

NF was defined with the following criteria: 1) fibrosis composed of proliferating myofibroblasts and/or collagen fibers, with or without tumor cells, 2) located within the tumor with a size of 5 mm or more in diameter. Fibrosis after preoperative fine needle aspiration cytology could be excluded with these criteria.

Multifocality was defined as the presence of additional tumor foci noncontiguous to the primary tumors in the resected thyroid specimens. Extrathyroidal invasion (Ex) was the extension of tumor beyond the thyroid capsule to the perithyroidal tissue. Ex was divided into the following three grades (Ex0 - 2) using the classification of The Japanese Society of Thyroid Surgery (13) as follows: Ex0, invasion does not exceed thyroid capsule; Ex1, invasion exceeds thyroid capsule but remains in sternothyroid muscle or adipose tissue; Ex2, invasion reaches other organ (trachea, larynx,

esophagus, recurrent nerve, carotid artery, internal jugular vein, and subcutaneous tissue).

Estimation of vascular invasion of cancer cells was carried out observing 4-um-thick histologic sections of the largest cut surface of formalin-fixed, paraffin-embedded blocks with double staining of hematoxylin eosin and elastica van Gieson. One focus of vascular invasion per one histologic section was scored as V1, and two foci or more as V2.

In addition, inflammation status (chronic lymphocytic thyroiditis) of background thyroid tissue was examined in each case according to the criteria of Williams and Doniach (14,15); grade 0, 0-1 focus per standard representative section (2 cm^2); grade 1, 2-8 foci per standard representative section; grade 2, 9-40 foci per standard representative section; grade 3, more than 40 foci per standard representative section; and grade 4, more than half of the glandular parenchyma replaced in a standard representative section. A 'focus' was defined as an aggregate of 50 or more lymphocytes. A nontumorous region was selected at least 5mm from the borderline with the tumor to avoid reactive lymphoid cell infiltration around the tumor.

Immunohistochemistry

Formalin-fixed and paraffin-embedded blocks of cancer lesions were selected. For the case of PAP with IHO, the blocks adjacent to ossification but without ossification were used to avoid the influence of decalcification process on immunohistochemistry. Immunostaining was achieved on the largest section of each tumor. The used primary antibodies are listed in Table 1. While Envision + system (Dako, Glostrup, Denmark) was used for the primary antibodies against αSMA, bFGF, vascular endothelial growth factor (VEGF), CD34, and nestin, LSAB+ system-HRP (Dako) was applied for the antibody against BMP-2. Chromogenic fixation was carried out by immersing the sections in 3,3'-diaminobenzidine solution. Counterstaining was carried out with Mayer's hematoxylin.

Immunohistochemical Examination

Immunohistochemical reactivity was evaluated blindly without knowledge of the clinicopathological information.

Myofibroblast counting was performed immunohistochemically using αSMA- stained slides. αSMA-positive fibroblastic cells in intratumoral

stroma were considered as myofibroblasts. The immunostained sections were scanned by light-microscopy at low magnification (×40) and the areas with the greatest number of distinctly highlighted αSMA-positive fibroblastic spindle cells were selected. Then, the number of myofibroblasts was determined by counting all immunostained myofibroblasts in five areas at a magnification of ×200 for each case using ocular micrometer. The mean number of myofibroblasts in a field of 0.25 mm^2 in each case was then calculated, and defined as myofibroblast count (MFC) in tumor. For PAP with IHO and PAP with NF cases, both tumor and NF areas were evaluated independently. In follicular carcinoma, fibrosis was hardly observed. Therefore, we examined only papillary carcinoma.

For bFGF, BMP-2, and VEGF, the stained slides were examined microscopically using the following parameters and semiquantitative criteria. Cytoplasmic immunostaining intensity in both tumor cells and stained area was evaluated. The intensity of the immunoreaction was classified into 4 levels: 0, no staining; 1, weak staining; 2, moderate staining; and 3, strong staining. In addition, the percentage of immunoreactive cancer cells was recorded: 0, negative; 1, 1% to 25%; 2, 26% to 50%; 3, 51% to 75%; and 4, 76%

to 100%. Both scores were multiplied to generate a total score of 0 to 12, according to Sinicrope's method (16).

CD34-expressing capillaries were counted to give the microvascular density. Nestin-positive capillaries were considered as capillaries consisting of newly formed endothelial cells (17). In both immunostainings, areas of highest density of capillaries were found by scanning tumor sections at low power (×100). Then, the numbers of capillaries were counted in 5 different fields at high power (x400). The average number of capillaries per high-power field (x400) was defined as microvascular density with both immunostainings.

Statistical Analysis

Kruskal-Wallis test and Mann-Whitney U-test were used to test among more than 3 groups. Chi-square test was carried out to analyze categorical data. A computer program package (Stat View 5.0, Abacus Concepts, Berkeley, CA, USA) was used for all statistical tests and management of the database. A *P*-value less than 0.05 was considered to be significant.

Results

Clinicopathological Data

The histopathological variants (18) with number of cases and clinicopathological data for the examined cases are summarized in Table 2A and 2B. Most of cases of papillary thyroid carcinoma were conventional type (Table 2B). Cases of PAP with IHO all showed NF in the lesion, and the ossification was formed in the fibrotic area (Image 1).

The mean ages of PAP with IHO, PAP with NF, and PAP without NF were 59.1 ± 14.8, 57.5 ± 16.9, and 51.7 ± 12.3, respectively. There was no difference between PAP with IHO and PAP with NF. Ages in both cases of PAP with IHO and PAP with NF were significantly greater than those in cases of PAP without NF ($P = 0.015$, $P = 0.004$, respectively). The mean size of each group of papillary thyroid carcinoma was not significantly different. FC was larger than any group of thyroid carcinoma ($P<0.0001$, $P<0.0001$, $P<0.0001$, respectively).

Calcification existed in 48 cases of PAP with IHO (100%), 4 cases of PAP with NF (15%), 4 cases of PAP without NF (12%), and 2 cases of FC (6%). The

incidence in PAP with IHO was significantly greater than that in PAP with NF or PAP without NF ($P < 0.001$).

Multifocality was identified in 40 cases of PAP with IHO (83%), 19 cases of PAP with NF (73%), and 18 of PAP without NF (53%). PAP with IHO showed higher incidence than PAP without NF ($P = 0.003$) for multifocality.

Lymph node dissection was carried out in 113 patients. Cases of both PAP with IHO and PAP with NF showed significantly higher incidence of lymph node metastasis than cases of PAP without NF ($P = 0.0025$, $P = 0.0165$, respectively). Similarly, Ex was more frequent in PAP with IHO and PAP with NF than in PAP without NF ($P < 0.0001$, $P < 0.0001$, respectively).

Chronic lymphocytic thyroiditis in background thyroid tissue was assessed and summarized in Table 3. There were no significant differences among the 3 groups of PAP (p=0.067)

Myofibroblast Counting (MFC)

Immunoreactive αSMA was positive in stromal myofibroblasts (Image 2). MFC in tumor area, PAP with IHO, and PAP with NF possessed significantly higher levels of myofibroblasts than PAP without NF ($P = 0.017$,

$P = 0.004$, respectively) (Figure 1A). As for MFC in NF, PAP with NF had more myofibroblasts than PAP with IHO ($P = 0.002$) (Figure 1B).

bFGF and BMP-2 Protein Expression

bFGF was expressed in the cytoplasm and nucleus of cancer cells (Image 3A, 3D). BMP-2 was localized in the cytoplasm of cancer cells (Image 3B, 3E). Both bFGF and BMP-2 showed strong positivity in cancer cells around fibroblastic foci (Image 3A, 3B). Both bFGF and BMP-2 expressions were higher in papillary carcinoma than in follicular carcinoma. bFGF score of PAP with IHO was the highest in papillary carcinoma, with PAP with NF showing intermediate levels and PAP without NF having the lowest immunopositivity (Figure 2A). BMP-2 score had a similar pattern to bFGF score (Figure 2B).

VEGF Expression

VEGF expression in cancer cells was significantly higher in PAP with IHO and PAP with NF than in PAP without NF. No significant difference was

observed between PAP with IHO and PAP with NF (Image 3C, 3F, Figure 2C).

Vascular Invasion of Cancer Cells

Vascular invasion of cancer cells was identified by elastic van Gieson staining. Vascular permeation by cancer cells was frequently found in the order of PAP with IHO, PAP with NF, and PAP without NF, the difference between each group being significant (Table 2A).

Microvessel Density Identified by CD34 and Nestin

Microvascular density identified by CD34 showed no significant difference among the 3 groups of papillary carcinoma. On the other hand, microvascular density examined with nestin staining, which can identify newly formed capillaries, increased in the order of PAP without NF, PAP with NF, and PAP with IHO, the difference being significant (Image 3G-J, Figure 3).

Discussion

Regarding the ossification of thyroid carcinoma, no significant clinicopathological characteristics were previously reported. IHO was found in 23.1% of PAP cases (48 of 207). Although previous reports about the incidence of IHO were limited, Bai et al (2). reported the incidence as 16.0% (29 in 181 papillary carcinomas) and Yamashita et al (19). reported as 17.6% (6 in 34). These figures showed no significant difference between our figure ($p=0.101$, $p=0.619$, respectively). IHO was not found in any cases of follicular carcinoma, indicating that IHO was a specific feature in papillary thyroid carcinomas. The clinicopathological examination of the present study, for the first time, revealed that PAP with IHO showed high incidences of multifocality, lymph node metastasis, and extrathyroidal invasion. IHO was revealed to be tightly associated with intratumoral nodular fibrosis (NF), but not associated with chronic lymphocytic thyroiditis. Therefore, we focused our attention on the mechanism of how the stromal fibrosis is induced in papillary carcinoma lesion, and how IHO starts in association with fibrosis.

The presence of stromal myofibroblasts in PAP with IHO and PAP with NF was detected by immunohistochemical examination as αSMA-positive

spindle cells in the stroma, particularly in NF. MFCs in cases with IHO and with NF were significantly higher than in cases without NF. In addition, regarding MFC in NF, PAP with NF had more myofibroblasts than PAP with IHO. We consider that nodular fibrotic area hyalinizes as time goes by, and heterotopic ossification occurs in the old fibrotic region.

Tissue integrity is generally maintained by the stroma. In cancer, however, tumor cell invasion is driven by the stroma (4). Myofibroblasts and cancer-associated fibroblasts are important components of the tumor stroma (20). Myofibroblastic stroma has been reported to correlate with poor prognosis in several tumor types, including breast (21,22), colorectal (23), and oral cancers (24). A high level of myofibroblastic stroma has been reported to be associated with local recurrence (22). αSMA-positive myofibroblastic stroma may serve as a general marker of carcinoma aggressiveness, although it is not yet clear why certain tumors develop this stroma. The origin of myofibroblasts of tumor stroma remains controversial, although local fibroblasts and bone marrow-derived precursors are considered to be the main progenitor cells (20).

The mutual interaction between cancer cells and myofibroblasts depends on many invasive growth-promoting factors, through direct cell-cell contacts and paracrine signals (3). We found here a trend of the highest expression of bFGF and BMP-2 in PAP with IHO.

bFGF was suggested to participate in tumor invasion, fibroblastic stromal reaction, and lymph node metastasis. bFGF can stimulate proliferation and differentiation of fibroblasts and vascular endothelial cells (6,7). Recent studies have shown that bFGF are overexpressed in various cancers, such as lung cancer (25), breast cancer (26), and colon cancer (27), demonstrating a close association with angiogenesis, as well as with the progress of cancer. Previous studies of thyroid carcinoma reported a trend of higher expression of bFGF in carcinomas than in benign proliferative lesions, and in benign lesions than in normal tissue (28). However, there were no reports of the relationship among bFGF expression, stromal fibrosis, and IHO.

TGF-β is the most potent cytokine driving myofibroblast transdifferentiation (4). BMP-2 is a member of the TGF-β superfamily (9). BMP-2 was originally described as a protein that can induce ectopic bone formation (8). Immunohistochemical studies using anti-BMP-2 antibody for

heterotopic ossification associated with neoplasms have been reported in lungs (29). IHO in papillary thyroid carcinoma is more frequently seen than that in other organ carcinomas. Thus, BMP-2 expression in the carcinoma cells was considered to be important for the IHO.

PAP with IHO was found to show a higher level of neovascularization, shown by nestin-positive microvascular density, than other groups. Recent reports indicated that intratumoral lymphatics in papillary thyroid carcinomas was associated with lymph node metastasis (30), and that VEGF expression in papillary carcinoma cells correlated with lymph node metastasis (31,32). Since anti-VEGF antibody used in our immunohistochemical study was produced by immunization with the N-terminus of VEGF-A, simple comparison of our results with those of previous reports (29,30) was difficult. However, frequent lymph node metastasis in PAP with IHO can be explained by our results.

In our series, only 1 case of follicular variant PAP was included. In literatures from Western world, the incidence of follicular variant is much higher. Follucular variant occupied 20% to 38% of PAP cases (33,34). However, much lower figures were reported from Aaia. In a report of Zhu et

al (35). from China, follicular variant PAP was 7 cases (4.5%) of total 155 PAP cases. There was no significant difference between their figures and ours ($p=0.192$). Althoug the reason of the difference between Western world and Asia is unknown, Racial difference might influence the incidence.

Follicular carcinomas were also immunohistochemically examined in this study. From the results of bFGF, BMP-2, and VEGF, follicular carcinoma was considered to be clearly different from papillary carcinoma.

In conclusion, PAP with IHO showed frequent lymph node metastasis, multifocality, and extrathyroidal invasion. It is considered that bFGF produced by carcinoma cells stimulates myofibroblast proliferation, which results in NF, and that old NF shows ossification induced by BMP-2 from carcinoma cells. Such carcinoma cells tend to produce VEGF, which leads to neovascularization and lymphatic invasion (Figure 4). Thus, PAP with IHO should be regarded as a unique subtype of thyroid carcinoma.

References

1. Lu Z, Mu Y, Zhu H, Luo Y, Kong Q, Dou J, *et al.* Clinical value of using ultrasound to assess calcification patterns in thyroid nodules. World J Surg 2011;35:122-127.

2. Bai Y, Zhou G, Nakamura M, Ozaki T, Mori I, Taniguchi E, *et al.* Survival impact of psammoma body, stromal calcification, and bone formation in papillary thyroid carcinoma. Mod Pathol 2009:22:887-894

3. Worthley DL, Giraud AS, Wang TC. Stromal fibroblasts in digestive cancer. Cancer Microenviron 2010;3:117-125.

4. De Wever O, Mareel M. Role of tissue stroma in cancer cell invasion. J Pathol 2003;200:429-447.

5. Inoue Y, King TE, Jr., Barker E, Daniloff E, Newman LS. Basic fibroblast growth factor and its receptors in idiopathic pulmonary fibrosis and lymphangioleiomyomatosis. Am J Respir Crit Care Med 2002;166:765-773.

6. Dailey L, Ambrosetti D, Mansukhani A, Basilico C. Mechanisms underlying differential responses to FGF signaling. Cytokine Growth Factor Rev 2005;16:233-247.

7. Ribatti D, Vacca A, Rusnati M, Presta M. The discovery of basic fibroblast growth factor/fibroblast growth factor-2 and its role in haematological malignancies. Cytokine Growth Factor Rev 2007;18:327-334.

8. Wozney JM, Rosen V, Celeste AJ, Mitsock LM, Whitters MJ, Kriz RW *et al.* Novel regulators of bone formation: molecular clones and activities. Science 1988;242:1528-1534.

9. Chen D, Zhao M, Mundy GR. Bone morphogenetic proteins. Growth Factor 2004;22:233-241.

10. Clement JH, Marr N, Meissner A, Schwalbe M, Sebald W, Kiche KO, *et al.* Bone morphogenetic protein 2 (BMP-2) induces sequential changes of Id gene expression in the breast cancer cell line MCF-7. J Cancer Res Clin Oncol 2000;126:271-279.

11. Bieniasz M, Oszajca K, Eusebio M, Kordiac J, Bartkowiak J, Szemrai J. The positive correlation between gene expression of the two angiogenic factors: VEGF and BMP-2 in lung cancer patients. Lung Cancer 2009;66:319-326.

12. Hardwick JC, Van Den Brink GR, Bleuming SA, Ballester I, Van Den Brande JM, Keller JJ, *et al.* Bone morphogenetic protein 2 is expressed by, and acts upon, mature epithelial cells in the colon. Gastroenterology 2004;126:111-121.

13. The Japanese Society of Thyroid Surgery. General rules for the description of thyroid cancer. 5th edn. Kanehara: Tokyo; 1996.

14. Williams ED, Doniach I. The post-mortem incidence of focal thyroiditis. J Pathol Bacteriol 1962;83:255-264.

15. Okayasu I, Fujiwara M, Hara Y, Tanaka Y, Rose NR. Association of chronic lymphocytic thyroiditis and thyroid papillary carcinoma. A study of surgical cases among Japanease, and white and African Americans. Cancer 1995;76:2312-2318.

16. Sinicrope FA, Ruan SB, Cleary KR, Stephens LC, Lee JJ, Levin B. bcl-2 and p53 oncoprotein expression during colorectal tumorigenesis. Cancer Res 1995;55:237-241.

17. Teranishi N, Naito Z, Ishiwata T, Tanaka N, Furukawa K, Seya T, *et al.* Identification of neovasculature using nestin in colorectal cancer. Int J Oncol 2007;30:593-603.

18. DeLellis RA, Lloyd RV, Heitz PU. Pathology and genetics of tumours of endocrine organs (World Health Organization classification of tumours; 8). IARC Press, Lyon , 2004.

19. Yamashita H, Noguchi S, Murakami N, Tuji K, Yamaoka N, Sakamoto A. DNA ploidy and stromal bone formation as prognostic indicators of thyroid papillary carcinoma in aged patients: A retrospective study. Acta Pathologica Japonica 1993;43:22-27.

20. De Wever O, Demetter P, Mareel M, Bracke M. Stromal myofibroblasts are drivers of invasive cancer growth. Int J Cancer 2008;123:2229-2238.

21. Trojan L, Thomas D, Knoll T, Grobholz R, Alken P, Michel MS. Expression of pro-angiogenic growth factors VEGF, EGF and bFGF and their topographical relation to neovascularisation in prostate cancer. Urol Res 2004;32:97-103.

22. Surowiak P, Murawa D, Materna V, Maciejczyk A, Pudelko M, Ciesla S, *et al.* Occurence of stromal myofibroblasts in the invasive ductal breast cancer tissue is an unfavourable prognostic factor. Anticancer Res 2007;27:2917-2924.

23. Tsujino T, Seshimo I, Yamamoto H, Ngan CY, Ezumi K, Takemasa I, *et al.* Stromal myofibroblasts predict disease recurrence for colorectal cancer. Clin Cancer Res 2007;13:2082-2090.

24. Kellermann MG, Sobral LM, da Silva SD, Zecchin KG, Graner E, Lopes MA, *et al.* Myofibroblasts in the stroma of oral squamous cell carcinoma are associated with poor prognosis. Histopathology 2007;51:849-853.

25. Behrens C, Lin HY, Lee JJ, Raso MG, Hong WK, Lotan R, *et al.* Immunohistochemical expression of basic fibroblast growth factor and fibroblast growth factor receptors 1 and 2 in the pathogenesis of lung cancer. Clin Cancer Res 2008;14:6014-6022.

26. Faridi A, Rudlowski C, Biesterfeld S, Schuh W, Rath W, Schroder W. Long-term follow-up and prognostic significance of angiogenic basic fibroblast growth factor (bFGF) expression in patients with breast cancer. Pathol Res Pract 2002;198:1-5.

27. Elagoz S, Egilmez R, Koyuncu A, Muslehiddinoglu A, Arici S. The intratumoral microvessel density and expression of bFGF and nm23-H1 in colorectal cancer. Pathol Oncol Res 2006;12:21-27.

28. de la Torre NG, Buley I, Wass JA, Tuner HE. Angiogenesis and lymphangiogenesis in thyroid proliferative lesions: relationship to type and tumour behaviour. Endocr Relat Cancer 2006;13:931-944.

29. Kuribayashi H, Tsuta K, Mizutani E, Maeshima AM, Yoshida Y, Gemma A, *et al.* Clinicopathological analysis of primary lung carcinoma with heterotopic ossification. Lung Cancer. 2009;64:160-165.

30. Hall FT, Freeman JL, Asa SL, Jackson DG, Beasley NJ. Intratumoral lymphatics and lymph node metastasis in papillary thyroid carcinoma. Arch Otolaryngol Head Neck Surg 2003;129:716-719.

31. Yu XM, Lo CY, Chan WF, Lam KY, Leung P, Luk JM. Increased expression of vascular endothelial growth factor C in papillary thyroid carcinoma correlateds with cervical lymph node metastases. Clin Cancer Res 2005;11:8063-8069.

32. Yasuoka H, Nakamura Y, Zuo H, Tang W, Takamura Y, Miyauchi A, *et al.* VEGF-D expression and lymph vessels play an important role for lymph node metastasis in papillary thyroid carcinoma. Mod Pathol 2005;18:1127-1133.

33. Ozdemir D, Ersoy R, Cuhaci N, Arpaci D, Ersoy EP, Korukluoglu B, *et al.* Classical and follicular variant papillary thyroid carcinoma: comparison of clinical, ultrasonographical, cytorogical, and historogical features in 444 patients. Endocr Pathol 2001;22:58-65.

34. Ceresini G, Corcione L, Michiara M, Sgargi P, Teresi G, Gilli A, *et al.* Thyroid cancer incidence by histological type and related variants in a mildly iodine-deficient area of northern Italy, 1998 to 2009. Cancer 2012;118:5473-5480.

35. Zhu X, Sun T, Lu H, Zhou X, Lu Y, Cai X, *et al.* Diagnostic significance of CK19, PET, galectin-3 and HBME-1 expression for papillary thyroid carcinoma. J Clin Pathol 2010;63:786-789.

6. 業績目録

（I）原　著

◎1. Takeda M, Mikami T, Numata Y, Okamoto M, Okayasu I : Papillary thyroid carcinoma with heterotopic ossification is a special subtype with extensive progression. Am J Clin Pathol, 139(5):587-598, 2013.

○2. Masaki T, Katada C, Nakayama M, Takeda M, Miyamoto S, Seino Y, Matsuba H, Okamoto T, Koizumi W, Tanabe S, Horiguchi S, Okamoto M, Muto M : Usefulness and pitfall of Narrow band imaging combined with magnifying endoscopy for detecting an unknown head and neck primary site with cervical lymph node metastasis. Auris Nasus Larynx, 39(5):502-506, 2012.

3. Nakayama M, Okamoto M, Seino Y, Miyamoto S, Hayashi S, Masaki T, Yokobori S, Takeda M. Inverted epiglottis: a postoperative complication of supracricoid laryngectomy with cricohyoidoepiglottopexy. Auris Nasus Larynx, 37(5):609-614, 2010.

○4. Nakayama M, Holsinger C, Okamoto M, Seino Y, Miyamoto S, Takeda M, Yokobori S, Masaki T, Hayashi S. Clinicopathological analyses of fifty supracricoid laryngectomized specimens: evidence base supporting minimal margins. ORL J Otorhinolaryngol Relat Spec, 71(6):305-311, 2010.

5. Masaki T, Katada C, Nakayama M, Takeda M, Miyamoto S, Seino Y, Koizumi W, Tanabe S, Horiguchi S, Okamoto M. Narrow band imaging in the diagnosis of intra-epithelial and invasive laryngeal squamous cell carcinoma: a preliminary report of two cases. Auris Nasus Larynx. 36(6):712-716.

6. Katada C, Nakayama M, Tanabe S, Koizumi W, Masaki T, Takeda M, Okamoto M, Saigenji K. Narrow band imaging for detecting metachronous superficial oropharyngeal and hypopharyngeal squamous cell carcinomas after chemoradiotherapy for head and neck cancers. Laryngoscope, 118(10):1787-1790, 2008.

7. Nakayama M, Okamoto M, Miyamoto S, Takeda M, Yokobori S, Masaki T, Seino Y. Supracricoid laryngectomy with cricohyoidoepiglotto-pexy or cricohyoido-pexy: experience on 32 patients. Auris Nasus Larynx, 35(1):77-82, 2008.

○8. 竹田昌彦、堅田親利、中山明仁、宮本俊輔、岡本牧人. Narrow Band Image (NBI) 内視鏡アシスト下に経口腔法切除した中咽頭癌の 2 症例. 頭頸部癌, 33(4):470-475, 2007.

○9. 竹田昌彦、中山明仁、宮本俊輔、岡本牧人. 経口腔法による側壁型中咽頭癌の手術治療 ーTransoral Lateral Oropharyngectomy についてー. 頭頸部癌, 32(4):468-473, 2006.

（Ⅱ）総説・講座

1. 竹田昌彦, 岡本牧人, 小田博雄: 小児の SAS 成人との差. ENTONI, 52: 1-6, 2005.

2. 竹田昌彦, 西山耕一郎, 岡本牧人: UPPP 我々の方法. 耳鼻咽喉科・頭頸部外科, 75(9): 611-615, 2003.

3. 竹田昌彦, 岡本牧人: 閉塞型 SAS(OSAS) 治療 手術療法. Pharma Medica, 21(10): 51-55, 2003.

（Ⅲ）症例報告

1．西山耕一郎、山中盾、廣島屋孝、横堀学、竹田昌彦、広瀬肇、岡本牧人: 舌根部甲状腺の有茎多植治療の１例. 日本耳鼻咽喉科学会報, 103: 770ー773, 2000.

Table 1. Primary antibodies used for immunohistochemistry

Antibodies	*Clonality*	*Pretreatment*	*Dilution*	*Supplier*
α-SMA (1A4)	Mouse monoclonal	—	1:1000	Dako, Glostrup, Denmark
bFGF (147)	Rabbit polyclonal	MW-CB	1:400	Santa Cruz Biotechnology, Santa Curz, CA
BMP-2 (N-16)	Rabbit polyclonal	MW-CB	1:100	Santa Cruz Biotechnology, Santa Curz, CA
VEGF (A-20)	Rabbit polyclonal	MW-CB	1:100	Santa Cruz Biotechnology, Santa Curz, CA
CD34 (QBEnd10)	Mouse monoclonal	—	1:500	Dako, Glostrup, Denmark
Nestin (18741)	Rabbit polyclonal	—	1:250	IBL, Takasaki, Japan

MW-CB, microwave in 0.01 mol/L citrate buffer (pH 6.0)

Table 2a. Histological variants of the cases of thyroid papillary carcinoma

	n	Variant types
Pap with IHO	41	Conventional type
	6	Encapsulated variant
	1	Tall cell variant
Pap with NF	22	Conventional type
	1	Encapsulated variant
	1	Follicular variant
	1	Tall cell variant
	1	Warthin tumor-like
Pap without NF	31	Conventional type
	2	Oncocytic variant
	1	Clear cell variant

Table 2b. Clinicopathological data of the thyroid carcinoma cases in view of ossification and fibrosis

	n	*Mean age (yr)*	*Size (mm)*	*Calcification*	*Multifocality*	*LNM*	*Ex*	*Vascular invasion*
Pap with IHO	48	59.1±14.8	25.9±10.2	48 (100%)	40 (83%)	38 / 46 (83%)	Ex0 10 (21%) Ex1 24 (50%) Ex2 14 (29%)	V0 11 (23%) V1 5 (10%) V2 32 (67%)
Pap with NF	26	57.5±16.9	30.2±16.3	4 (15%)	19 (73%)	21 / 26 (81%)	Ex0 4 (21%) Ex1 12 (46%) Ex2 10 (39%)	V0 5 (19%) V1 9 (35%) V2 12 (46%)
Pap without NF	34	51.7±12.3	26.3±17.0	4 (12%)	18 (53%)	15 / 30 (50%)	Ex0 26 (76%) Ex1 6 (18%) Ex2 2 (6%)	V0 21 (62%) V1 9 (26%) V2 4 (12%)
FC	33	47.3±16.6	50.1±19.0	2 (6%)	0 (0%)	1 / 11 (9%)	Ex0 33 (100%)	V0 12 (36%) V1 16 (48%) V2 5 (16%)

n, number of cases; IHO, intratumoral heterotopic ossification; NF, nodular fibrosis; FC, follicular carcinoma; LNM, lymph node metastases; Ex, extraglandular invasion; *, $P < 0.05$; †, $P < 0.01$

Table 3. The grade of chronic lymphocytic thyroiditis in background thyroid tissue.

	n	Grade 0	Grade 1	Grade 2
PAP with IHO	47	39	2	6
PAP with NF	26	17	0	9
PAP without NF	34	20	3	11
FC	33	31	1	1

n, number of cases; PAP, papillary carcinoma; IHO, intratumoral heterotopic ossification; NF, nodular fibrosis; FC, follicular carcinoma

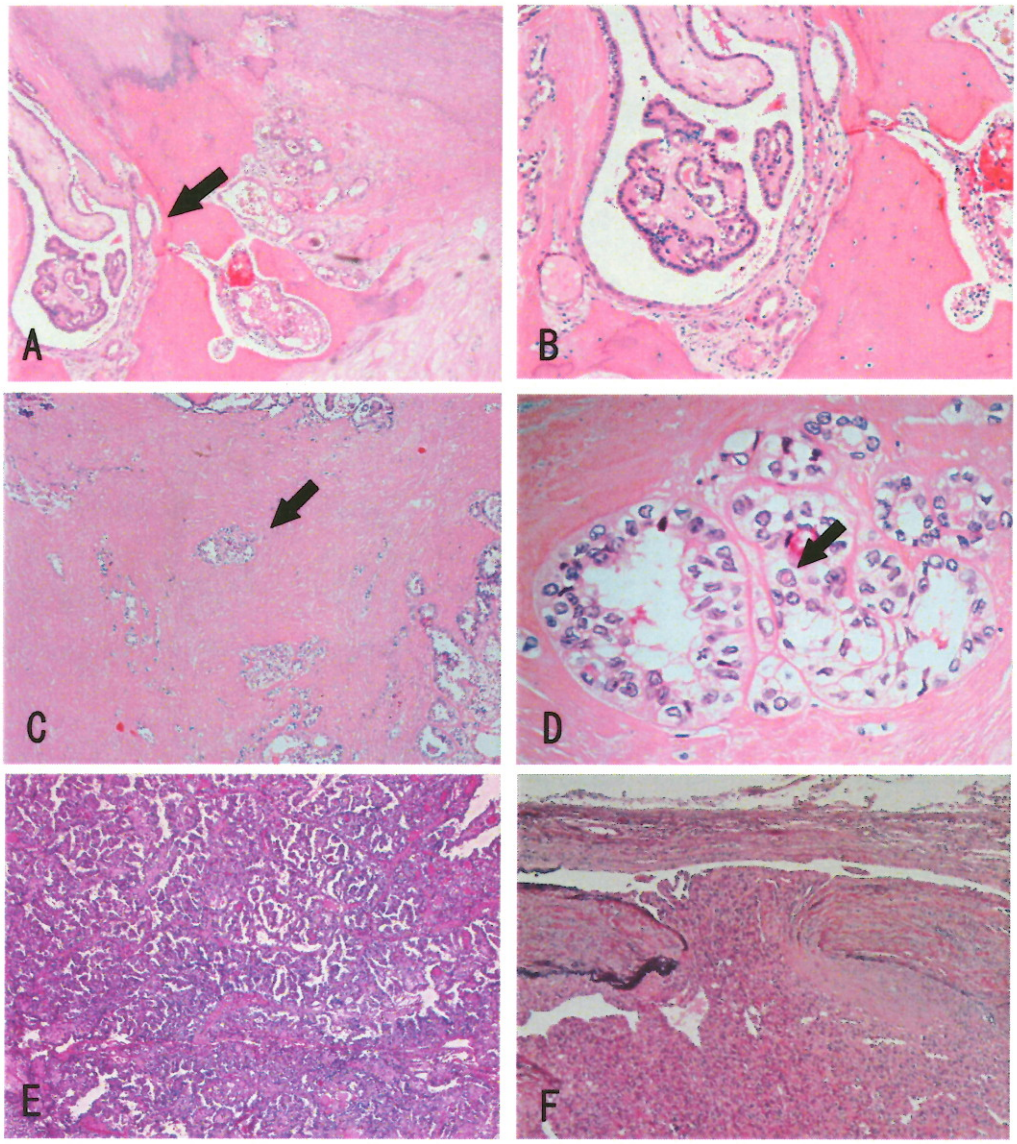

Image 1

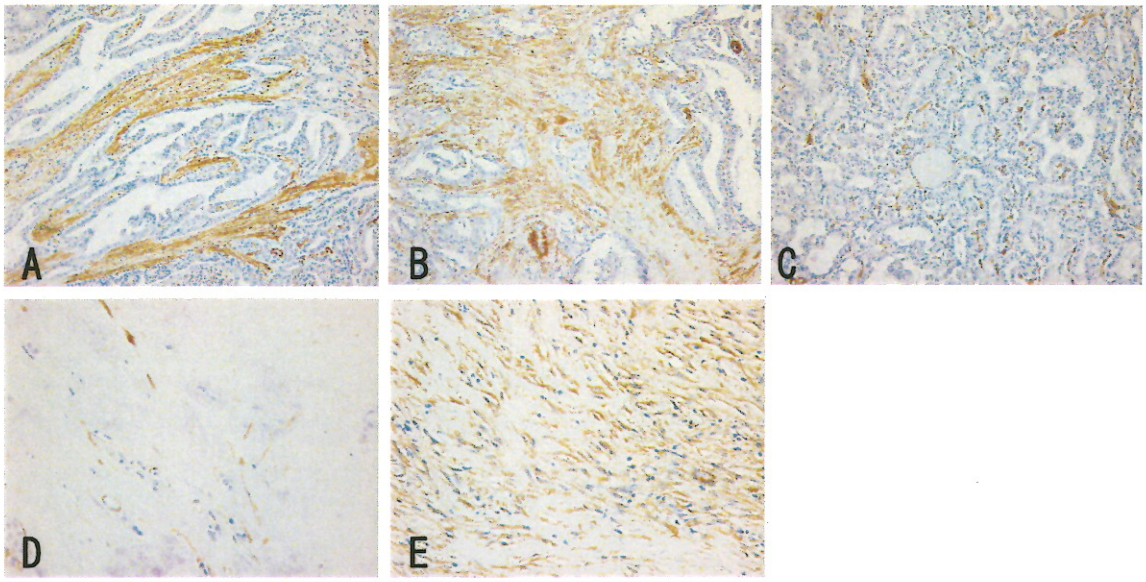

Image 2

Takeda et al

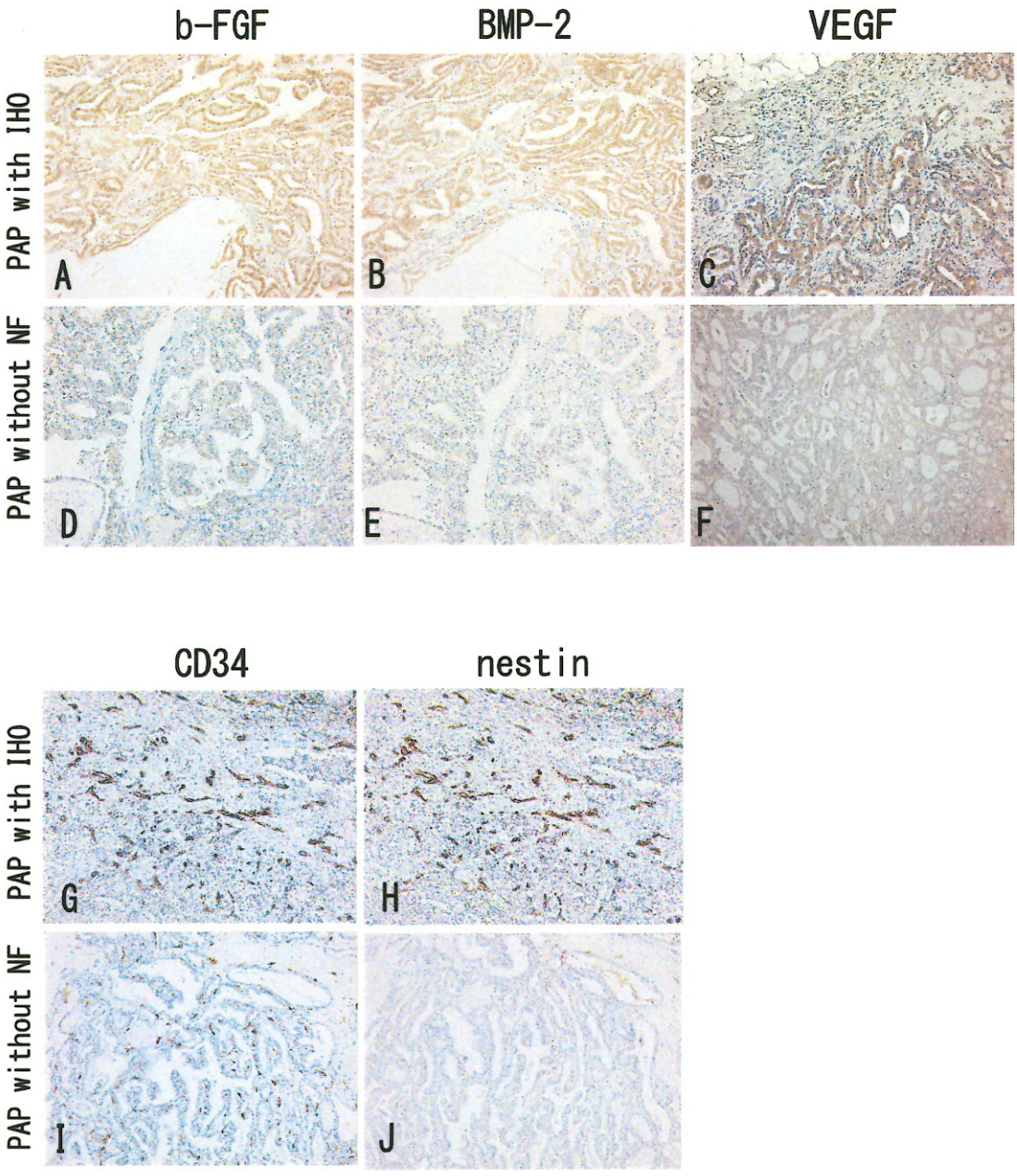

Image 3

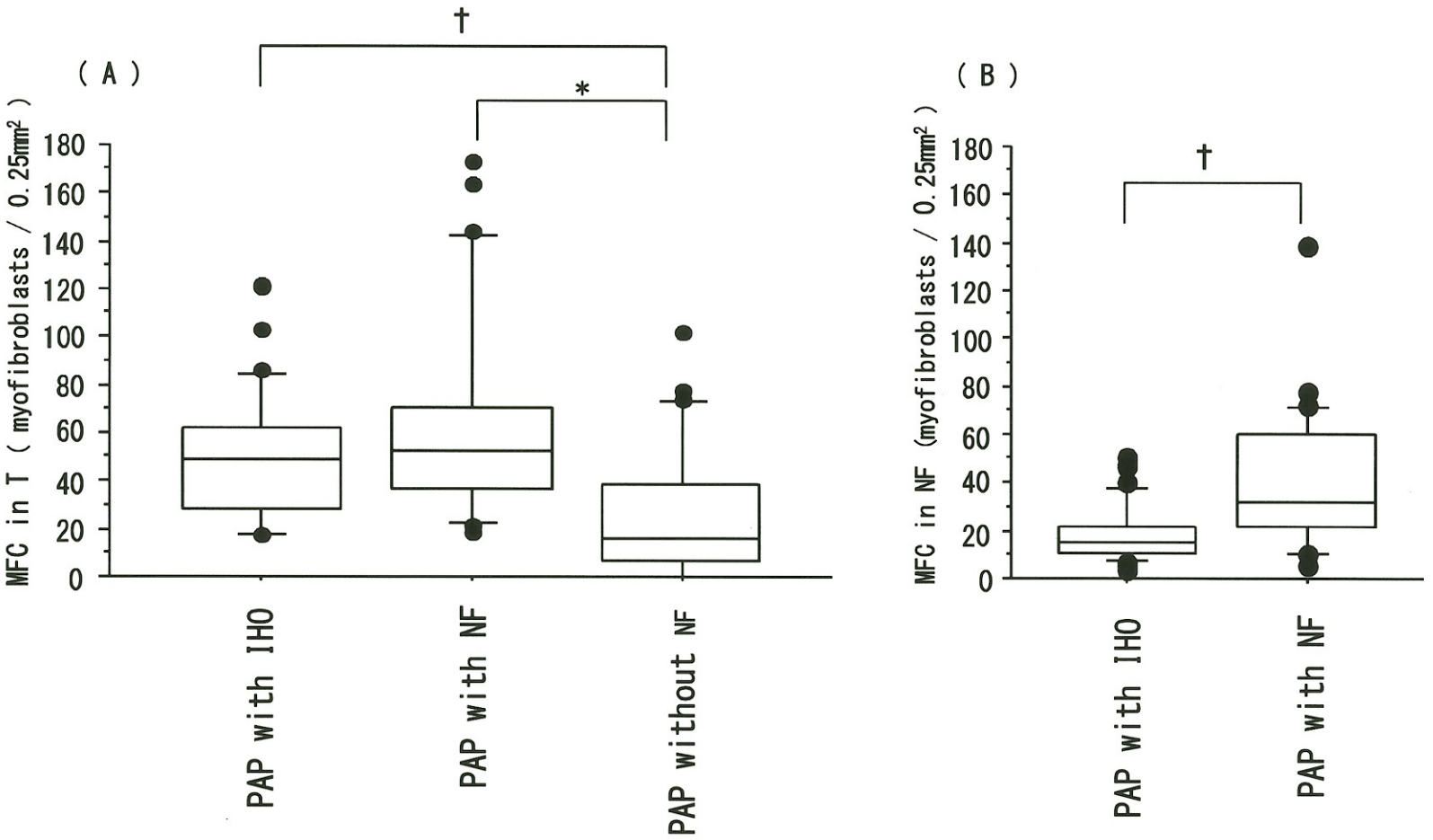
(A)
MFC in T (myofibroblasts / 0.25mm²)
180
160
140
120
100
80
60
40
20
0
†
*
PAP with IHO
PAP with NF
PAP without NF
(B)
MFC in NF (myofibroblasts / 0.25mm²)
180
160
140
120
100
80
60
40
20
0
†
PAP with IHO
PAP with NF

Figure 1

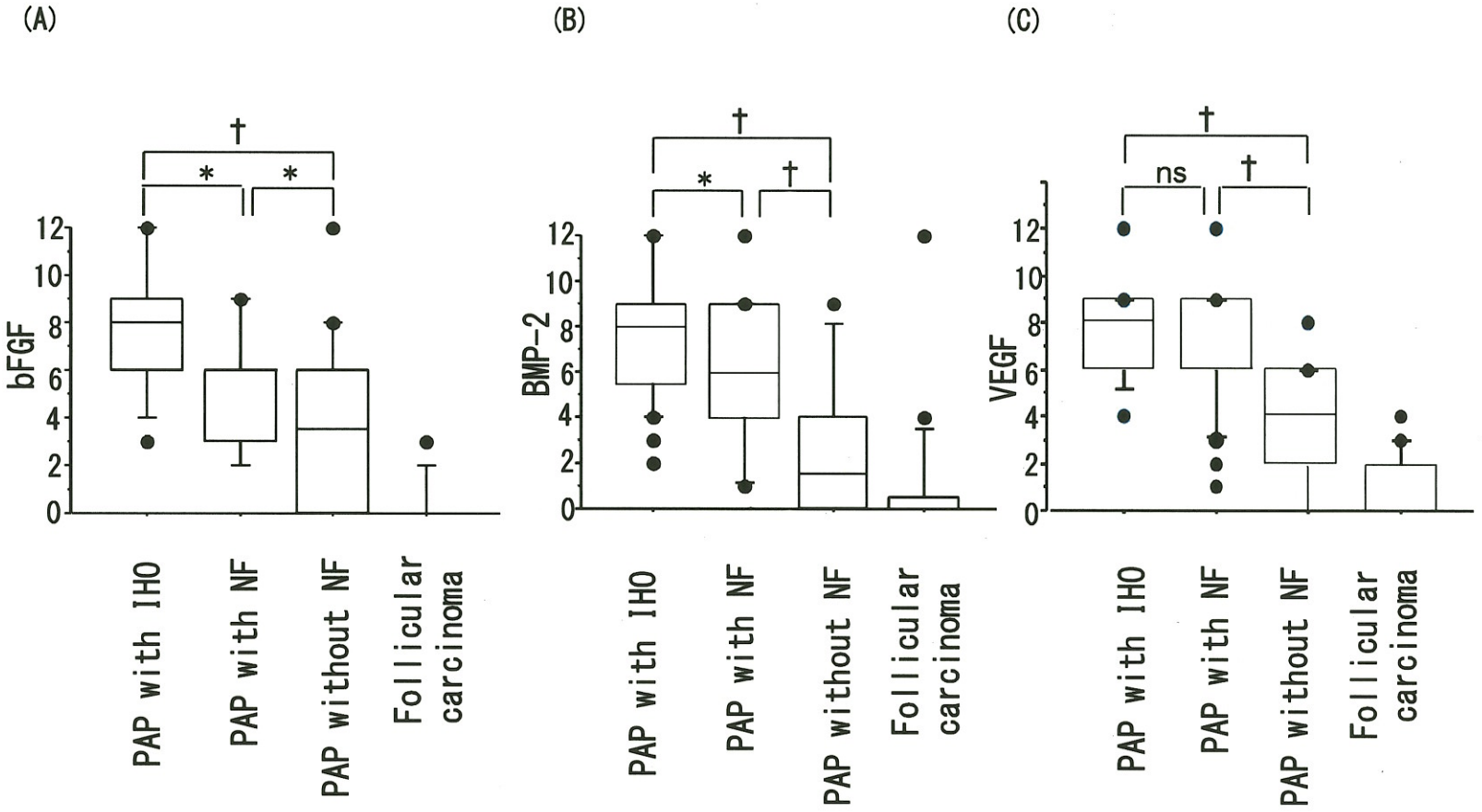
(A)
(B)
(C)
bFGF
BMP-2
VEGF
0
2
4
6
8
10
12
*
†
ns
PAP with IHO
PAP with NF
PAP without NF
Follicular carcinoma

Figure 2

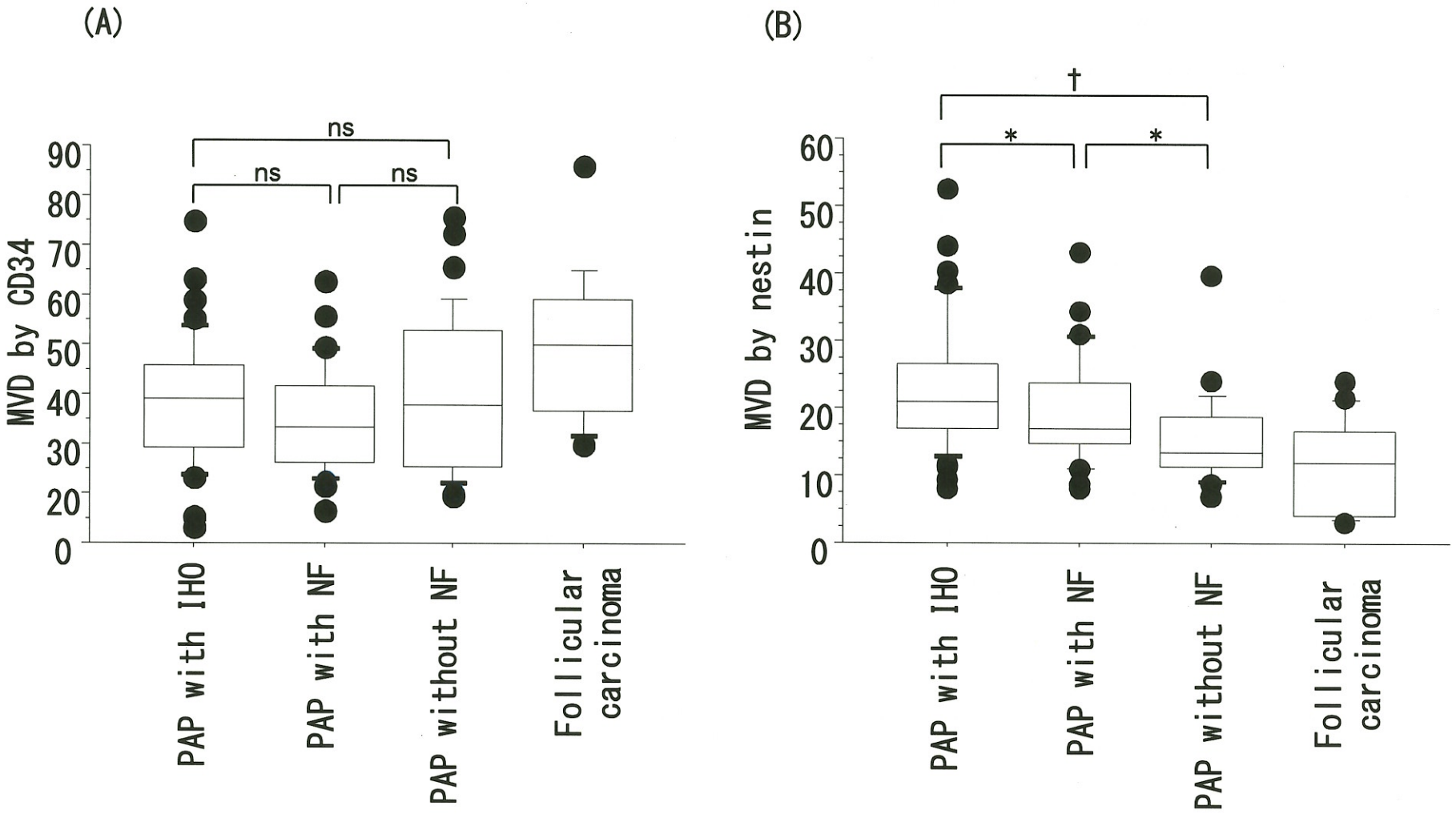
(A)
MVD by CD34
90
80
70
60
50
40
30
20
0
ns
ns
ns
PAP with IHO
PAP with NF
PAP without NF
Follicular carcinoma
(B)
MVD by nestin
60
50
40
30
20
10
0
†
*
*
PAP with IHO
PAP with NF
PAP without NF
Follicular carcinoma

Figure 3

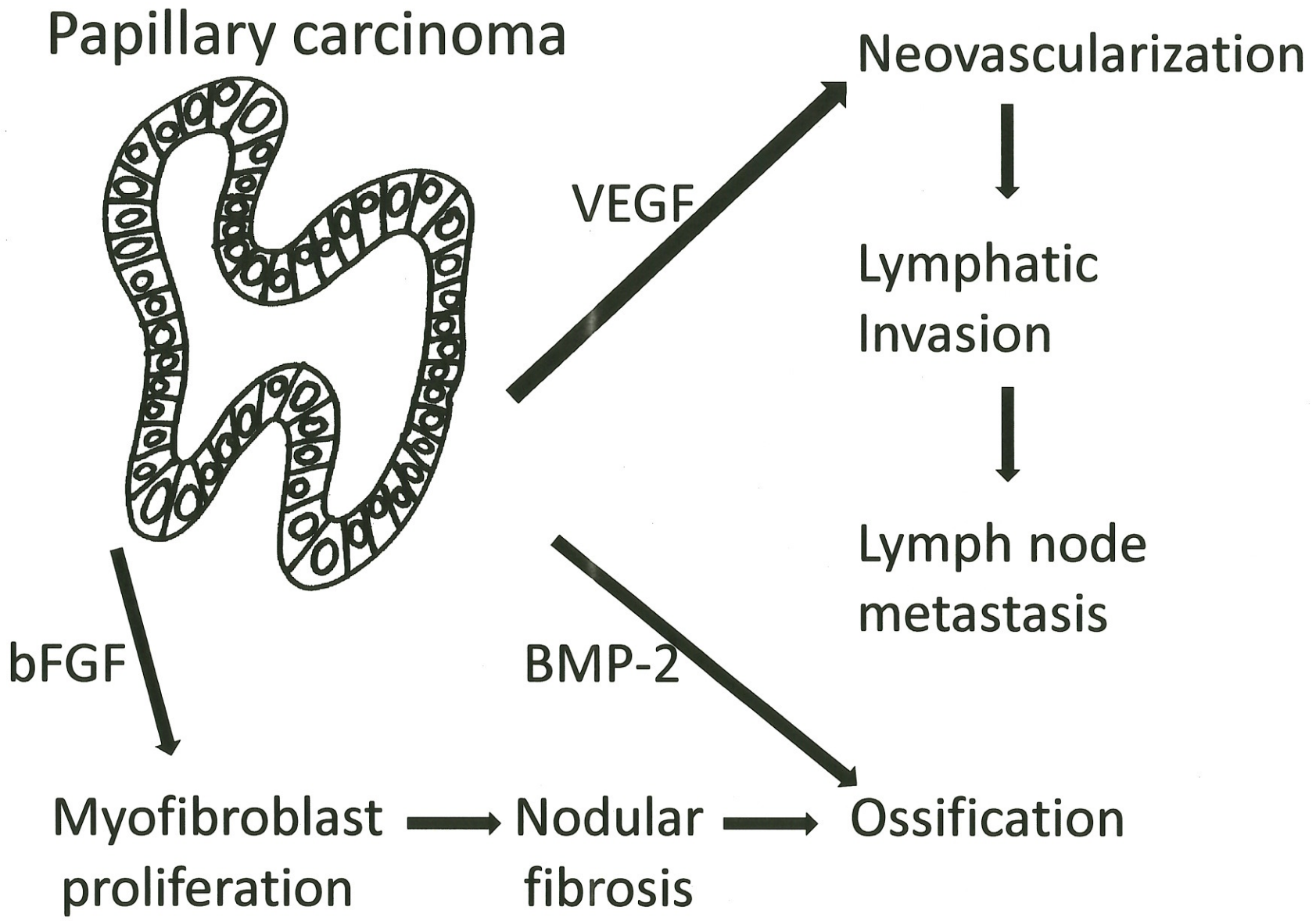
Papillary carcinoma
Neovascularization
VEGF
Lymphatic
Invasion
Lymph node
metastasis
bFGF
BMP-2
Myofibroblast
proliferation
Nodular
fibrosis
Ossification

Figure 4

Legends

Image 1 Subtypes of thyroid carcinomas. **(A)** PAP with IHO. An arrow indicates papillary carcinoma cells between bone trabeculae within NF. **(B)** Higher magnification of (A). **(C)** PAP with NF. Note prominent stromal fibrosis. An arrow indicates carcinoma cell nests. **(D)** Carcinoma cell nests in (C) in higher magnification. An arrow indicates a nucleus with pseudoinclusion. **(E)** PAP without NF. **(F)** Follicular carcinoma. Note capsular invasion of tumor cells.

Image 2 Representative α-smooth muscle actin (α SMA)–positive myofibroblasts. **(A)** cancer cells and α SMA^+ myofibroblast-rich stroma in a case of PAP with IHO, **(B)** cancer cells and α SMA^+ myofibroblast-rich stroma in a case of PAP with NF, and **(C)** cancer cells and α SMA^+ myofibroblast-poor stroma in a case of PAP without NF. **(D)** Hyalinized fibrotic (α SMA^+ myofibroblast-poor) stroma of the same case as **(A)**. **(E)** Fibrotic (α SMA^+ myofibroblast-rich) stroma of the same case as **(B)** .

Image 3 Basic fibroblast growth factor (bFGF), bone morphogenetic protein-2 (BMP-2), and vascular endothelial growth factor (VEGF) expression in papillary carcinoma. A case of PAP with IHO **(A, B, and C)**, and a case of PAP without NF **(D, E, and F)**. **(A)** Expression of b-FGF, **(B)** BMP-2, and **(C)** VEGF is remarkable in the tumor cells of PAP with IHO, while PAP without NF shows no expression of the 3 proteins **(D, E, and F)**.

Representative vascular channels immunostained with CD34 and nestin in a

case with PAP with IHO **(G,H)** and a case of PAP without NF **(I,J)**. Vascular channels immunostained with anti-CD34 are shown in both cases **(G,I)**. However, neovascularization immunostained with anti-nestin antibody is much more extensive in PAP with IHO **(H)** than in PAP without NF **(J)**.

Figure 1 Comparison of myofibroblast count (MFC) among PAP with IHO, PAP with NF, and PAP without NF. **(A)** MFC in tumor area. **(B)** MFC in NF area. $^{*}P < 0.05$, $^{\dagger}P < 0.01$.

Figure 2 Comparison of immunoreactive scores of **(A)** basic fibroblast growth factor (bFGF), **(B)** bone morphogenetic protein-2 (BMP-2), and **(C)** vascular endothelial growth factor (VEGF) among PAP with IHO, PAP with NF, and PAP without NF. $^{*}P < 0.05$, $\dagger P < 0.01$.

Figure 3 Comparison of microvascular density (MVD) and neovascularization examined with **(A)** CD34 and **(B)** nestin immunostaining among PAP with IHO, PAP with NF, and PAP without NF. $^{*}P < 0.05$, $\dagger P < 0.01$.

Figure 4 Schematic outline of our hypothesis about papillary carcinoma with intratumoral heterotopic ossification.